Analysis of the Triplet-state Kinetics of a Photosensitizer for Photoimmunotherapy by Fluorescence Correlation Spectroscopy

Hideo Takakura[a], Yuto Goto[a], Akira Kitamura[b], Toshitada Yoshihara[c], Seiji Tobita[c], Masataka Kinjo[b], Mikako Ogawa*[a]

[a] Laboratory of Bioanalysis and Molecular Imaging, Graduate School of Pharmaceutical Sciences, Hokkaido University, Sapporo, Hokkaido, 060-0812, Japan

[b] Laboratory of Molecular Cell Dynamics, Faculty of Advanced Life Science, Hokkaido University, Sapporo, Hokkaido, 001-0021, Japan

[c] Graduate School of Science and Technology, Gunma University, Kiryu, Gunma, 376-8515, Japan

*Corresponding author: Mikako Ogawa

Laboratory of Bioanalysis and Molecular Imaging, Graduate School of Pharmaceutical Sciences, Hokkaido University, Sapporo, Hokkaido 060-0812, Japan

Phone: +81-11-706-3767, Fax: +81-11-706-3767.

E-mail: mogawa@pharm.hokudai.ac.jp

Abstract

Herein, we evaluated the intersystem crossing quantum yield (Φ_{ISC}) of a silicon phthalocyanine derivatized from IRDye700DX (IR700) which is used as a photosensitizer for photoimmunotherapy (PIT), using fluorescence correlation spectroscopy (FCS). The calculated Φ_{ISC} was 0.019 ± 0.002. The FCS measurement was validated by experiment in the presence of potassium iodide, which can change the kinetics of the relaxation process in the excited state.

Keywords

Photoimmunotherapy, Silicon phthalocyanine, Intersystem crossing quantum yield, Fluorescence correlation spectroscopy, Triplet state

1. Introduction

IRDye700DX (IR700) (Fig. 1a) is a near infrared (NIR) dye used as a photosensitizer for NIR photoimmunotherapy (NIR-PIT), which is a new type of cancer therapy using the antibody-IR700 conjugate and NIR light.[1-3] The cytotoxicity is specifically induced for cancer cells, because the cell membrane is damaged when the conjugates are bound to the antigens of the cancer cell membrane and exposed to NIR

light.[4,5] In NIR-PIT, various tumor antigens, such as human epidermal growth factor receptor 2 (HER2) and epidermal growth factor receptor (EGFR), have been used for target molecules. It has been shown that in both *in vitro* and *in vivo* experiments, the effective cell death can be induced by NIR irradiation. Further, Phase I and II studies were successfully finished in 2017 (NCT02422979) and the following Phase III clinical trial in patients with head and neck cancers is ongoing worldwide. More recently, in Japan, Cetuximab-IR700 complex targeting for EGFR has been approved for the treatment of unresectable locally advanced or recurrent head and neck cancer. Thus, NIR-PIT should attract more attention in the future.

Currently, in PIT treatment, to maximize the efficiency, NIR light is delivered to deep sites in tumor with thin fibers, such as catheters or needles, because light is attenuated due to absorbance and scattering by tissue. Another strategy for the efficient activation of PIT reagents in deep sites is use of more light-sensitive photosensitizers which can be activated by less light dose. However, since PIT was first reported in 2011, only IR700 has been used as a photosensitizer for PIT and other photosensitizers have not been reported yet. Therefore, we do not know whether IR700 is the best photosensitizer for PIT. Recently, the cytotoxic mechanism of PIT has been reported; the excitation of IR700 by NIR light in the presence of electron donors induces cleavage of the axial ligand

on IR700 followed by the aggregation of conjugates, resulting in physical damage to the cell membrane (Fig. 1a).[6] This leads to tiny hole on cell membrane, inducing water inflow inside cells followed by cell swelling accompanied with blebs. Finally, immunogenic cell death occurs, which activates the host immunity against the targeted cancer cells. Thus, it is considered that in order to increase the light-sensitivity of photosensitizer, efficient cleavage of the axial ligand on IR700 by light irradiation is important. It is reported that cleavage of the axial ligand is promoted under hypoxic conditions.[6] Since oxygen is a triplet quencher,[7] a photoreaction that proceeds via the lowest triplet state (T_1) should be enhanced in the absence of oxygen. Thus, since the cell death in NIR-PIT is a spontaneous process after cell membrane damage, the cleavage of axial ligand on IR700 upon light irradiation was considered to proceed via the T_1 of IR700. This would be because electron transfer from the electron donor to the excited IR700 is more likely to occur due to longer lifetime of the T_1 of IR700 than first excited singlet state (S_1). Therefore, the T_1 of IR700 would be involved in the cleavage reaction rather than the S_1 (Fig. 1b), although this cleavage process is still unclear. Another cytotoxic mechanism of PIT is generation of cytotoxic singlet oxygen upon light exposure to IR700, which is also involved in the T_1 of IR700. Accordingly, in both cases, the T_1 of IR700 is important for cytotoxicity of PIT. In designing a next-generation photosensitizer for PIT, it would be beneficial to know the

intersystem crossing quantum yield (Φ_{ISC}) (from S_1 to T_1) of IR700. To date, however, the Φ_{ISC} of IR700 has never been evaluated. Herein, we report the Φ_{ISC} of an IR700 derivative obtained by means of fluorescence correlation spectroscopy (FCS). FCS is a single photon counting technique in which the fluctuations of fluorescence intensity are measured in a small detection volume by irradiation of a tightly focused laser beam in a large temporal dynamic range. Since the fluctuations result from various factors including photophysical effects on the fluorophore of interest, FCS provides information about the dynamic processes in the excited state, usually from sub-micro- to milli-seconds. Generally, the transitions to the triplet state can be detected as fluctuations of fluorescence signals because the triplet state is a long-lived (10^{-6}~10^{-3} s) and dark state in contrast to the short-lived (~10^{-9} s) and emissive singlet state (Fig. 1c, see Methods).[8-10] Φ_{ISC} is calculated by the obtained rate constant from S_1 to T_1 k_{isc} and lifetime τ_{FL} of the fluorophore in the singlet state using the following equation; $\Phi_{ISC} = k_{isc} \times \tau_{FL}$.

2. Materials and methods

2.1. Reagents.

Compound **1** was synthesized according to literature methods.[6] Potassium iodide (KI) was purchased from KANTO CHEMICAL Co., INC. (Tokyo, Japan).

2.2. FCS measurements

FCS measurements were performed using a ConfoCor 3 system combined with an LSM 510 META confocal laser scanning microscope (Carl Zeiss, Jena, Germany) through a C-Apochromat 40×/1.2 NA Korr UV-VIS-IR water-immersion objective (Carl Zeiss). A solution of 100 nM compound **1** in 0.1 M phosphate buffer (pH 7.0) in 8 well chambered cover glass (#155411; Thermo Fisher, Waltham, MA) was excited at 633 nm at different excitation irradiances. The confocal pinhole diameter was adjusted to 90 μm. The radius of pinhole projected to the sample space was 337 μm. To remove the detector-derived after pulsing noise, fluorescence was split using a half mirror (NT50/50) and detected after passing through a 655 nm long-pass filter (LP655) using two avalanche photodiode (APD) detectors. The pinhole position was adjusted as the position indicating the highest photon counts per molecule (CPM) of Cy5 solution. The cross-correlation function (CCF) was calculated and further analyzed as the autocorrelation function (ACF) of compound **1 as described in 2.7**. The same measurement was performed in the presence of 50 and 100 mM KI. Photon counts per molecule (CPM) of compound **1** were measured with different KI concentrations (0, 10, 50, 100 mM).

2.3. Fluorescent lifetime

The fluorescence decay of compound **1** in H_2O at 295 K was measured with a time-correlated single-photon counting system (Hamamatsu, Quantaurus-Tau C11367). The excitation source was a light-emitting diode (wavelength: 590 nm, pulse width: 0.9 ns, repetition frequency: 500 kHz). The fluorescence profile monitored at 685 nm was analyzed by deconvolution with the instrument response function to obtain the fluorescence lifetime.

2.4. Fluorescence quantum yield

The fluorescence quantum yield was measured with an absolute fluorescence quantum yield measurement system (Hamamatsu, C9920-01) which consists of a Xe arc lamp, a monochromator, an integrating sphere, and a multichannel detector. The excitation wavelength was 590 nm. The detail of this system is described elsewhere.[11]

2.5. Fluorescence spectrophotometry

Fluorescence spectroscopy measurements were performed using a spectrofluorometer (FP-8600, JASCO, Japan). A solution of 100 nM compound **1** in 0.1 M phosphate buffer (pH 7.0) was excited at 610 nm. The same measurements were

performed with various KI concentrations (10, 50, 100, 200, 300, 400, 500 mM).

2.6. Stern-Volmer plot

Fluorescence quenching is analyzed by the following Stern-Volmer equation,

$$\frac{F_0}{F} = 1 + k_q \tau_0 [Q]$$

$$K_{sv} = k_q \tau_0$$

where F_0 and F are the fluorescence intensities in the absence and presence of the quencher, respectively. k_q is the quenching rate constant describing bimolecular collisional deactivation of electronic energy and τ_0 is the fluorescence lifetime in the absence of quencher. [Q] is the concentration of the quencher. K_{sv} is the Stern-Volmer quenching constant.

2.7 Calculation of rate constants using FCS

The recorded ACFs ($G(\tau)$s) were fitted using a theoretical function for two-component three-dimensional (3D) diffusion with one-component exponential blinking dynamics (Eq. 1). The blinking population at equilibrium (T_{eq}) was the time- and space-averaged exponential relaxation fraction of IR700 within the detection volume; τ_T is the exponential relaxation time constant related to the blinking state.

$$G(\tau) = \frac{1}{N)} \sum_i^2 F_i \left(\frac{1}{1+\tau/\tau_{Di}}\right)\left(\frac{1}{1+s^2\tau/\tau_{Di}}\right)^{1/2} \times \frac{[1-T_{eq}+T_{eq}\exp(-\tau/\tau_T)]}{(1-T_{eq})} \quad \text{Eq. 1}$$

where N is the average number of fluorescent dyes in the detection volume; Fi is the i-th component fraction (i = 1 or 2); s is the structure parameter defining the 3D laser profile described as the ratio of ω_z and ω_0, the radius ω_0 and half-length ω_z are the distances at which the laser profile decreases to $1/e^2$ intensity [12 13]; The i-th characteristic diffusion time (τ_{Di}) for the fluorescent molecules is the passing through time in the detection volume. CPM was calculated using the sum of detected photon counts (mean count rate) in both APD detectors and N obtained from the curve fitting using Eq. 1. The structure parameter (s), which defines the ratio of ω_0 and ω_z, was obtained from 10 nM Cy5 solution measurement followed by a 3D diffusion model fitting (9.454 ± 1.044; mean ± SD; n = 7). The obtained s value prior to the IR700 measurement was fixed in all curve-fitting analysis in the same assay date. The ω_0 was obtained from both of known diffusion coefficient (360 μm^2/s) and measured diffusion time of Cy5 as above (273 ± 16.0 nm; mean ± SD; n = 7) by $\omega_0 = \sqrt{4D\tau_D}$. The calculated confocal volume in the experiments was 0.376 ± 0.082 fL (mean ± SD; n = 7). The laser power density at the focal plane was calculated using ω_0 and the measured value by laser power meter (LP10; Sanwa Electric Instrument, Tokyo, Japan).

T_{eq} and τ_T were given by following equations (2–3)[8,14]

$$T_{\mathrm{eq}} = \frac{k_{exc}k_{\mathrm{ISC}}}{k_{exc}(k_{\mathrm{ISC}}+k_T)+k_T(k_{FL}+k_{\mathrm{ISC}})} \quad \text{Eq. 2}$$

$$\tau_{\mathrm{T}} = k_{\mathrm{T}} + \frac{k_{exc}k_{\mathrm{ISC}}}{k_{exc}+k_{FL}} \quad \text{Eq. 3}$$

where k_{FL} is the deexcitation rate of S_1 to the ground state (S_0) given by fluorescence lifetime and fluorescence quantum yield; σ is the excitation cross section of compound **1** from S_0 to S_1; . k_{exc} is the activation rate of S_0 to S_1 given by $\sigma P_{\mathrm{exc}}/\varepsilon\pi\omega_0^2$, where P_{exc} is the applied laser irradiance; ε is the energy of photon represented by Planck's constant, excitation wavelength (633 nm), and the light speed. The fits of T_{eq} and τ_{T} as a function of applied laser irradiances gave the two rate constants for intersystem crossing k_{ISC} and for deexcitation of the triplet state k_{T} using the Solver add-in program in MS-Excel. The Φ_{ISC} was calculated with the k_{ISC}.

3. Result and discussion

In this study, we synthesized an IR700 dye without a conjugate linker on phthalocyanine (Pc) ring (**1**) (Fig. 1a) and performed the FCS measurement using compound **1** in a phosphate buffer (pH7.0). Fig. 2a shows the ACF curves of compound **1** excited by various laser powers. Upon laser irradiation, in addition to the amplitude derived from diffusion of compound **1**, the amplitude of the blinking relaxation process on a shorter time-scale (~10^{-6} s) was observed. The normalized ACF at the first data point,

0.2 μs gradually decreased as the excitation power was increased, indicating that the amplitude of a blinking population at equilibrium T_{eq} was getting higher. This means that the triplet state population was increased depending upon the excitation power. With high excitation power, the cycles of excitation-relaxation became faster due to the high energy density of the excitation light. Once the molecules in the singlet excited state are transferred to the triplet state, the molecules are retained in the triplet state off the cycle due to the longer lifetime, resulting in a high triplet state population under high excitation power. Plots of T_{eq} and the exponential relaxation rate against excitation irradiance were well fitted to the expression of the equations (Figs. 3a and 3b). The fits gave $k_{isc} = 3.8 \pm 0.3$ μs^{-1} and $k_T = 0.56 \pm 0.04$ μs^{-1} (mean ± S.D.; Table 1). With the lifetime of compound **1** $\tau_{FL} = 4.9$ ns, the calculated Φ_{ISC} was 0.019 ± 0.002. Since IR700 is almost same structure as compound **1**, the Φ_{ISC} of IR700 is expected to be similar. Further, we measured the fluorescence quantum yield (Φ_{FL}) of compound **1** and obtained 0.31, suggesting that internal conversion is the major relaxation process for compound **1** (Table 1).

Next, to investigate the validity of the FCS measurement, we checked whether we could detect the change of the photochemical property when the relaxation kinetic parameter of compound **1** was changed. For this purpose, we measured the blinking state of compound **1** in the presence of KI using FCS because triplet-state decay time constants

can change with the addition of KI; KI can promote intersystem crossing to the triplet state due to the heavy atom effect of the iodine atom (*i.e.* high k_{isc}), and it can enhance the triplet-state decay rate by a charge-coupled deactivation (*i.e.* high k_T).[15] In the ACF curve with 50 mM KI, the amplitude derived from the T_1 transition was observed, as was seen in the experiment lacking KI (Fig. 2b). In the T_{eq} plot, the T_{eq} was higher than that observed without KI even at the lower excitation power, suggesting that the addition of KI increased the blinking population (Fig. 3a). k_{isc} and k_T were obtained from the fitting analysis of T_{eq} and the exponential relaxation rate, showing that the k_{isc} was significantly increased, while the k_T was almost constant (Table 1). This means that KI enhanced the buildup of the triplet-state population of compound **1** due to the external heavy atom effect, but a charge-coupled deactivation effect was not observed. It is reported that the influence of KI on the triplet state parameters of fluorophores depends on the triplet energy level and the structure of the compounds and the charge-coupled interaction would be reduced by electric repulsion between the excited molecules and iodide anion.[15] Since compound **1** is highly negatively charged, it is speculated that the charge-coupled interaction with iodide anion did not occur. Moreover, in the FCS experiment with KI, we investigated the dependency of the brightness of compound **1** on KI concentration. The brightness of compound **1** decreased with increasing KI concentration (Fig. 4a). To evaluate the

quenching effect of KI, Stern-Volmer analysis, in which dynamic (collisional) or static quenching can be distinguished by the quenching rate constant, was examined using the fluorescence intensity obtained from a fluorescence spectrometer (Fig. 4b).[16] The fluorescence intensities of compound **1** decreased with increasing KI in the same manner as the FCS measurement. In the Stern-Volmer plot, the quenching constant K_{SV} = 6.2 L/mol was obtained, leading to the quenching rate constant $k_q = 1.4 \times 10^9$ L/mol·s (Fig. 4c). A diffusion rate constant in water is reported to be about 7×10^9 L/mol·s at room temperature.[17] Since obtained k_q is close to the diffusion rate constant in water, intermolecular dynamic quenching between compound **1** and iodide ion occurred, resulting in less photons of compound **1**. In addition of 50 mM KI, k_{ISC} was changed, but the quenching constants were underestimated comparing to that from Stern-Volmer plot. A possible explanation of the underestimation is maybe because we assume that the decay of the singlet state by fluorescence (k_{FL}) is much faster than either of the process of intersystem crossing or triplet state decay (*i.e.*, $k_{FL} >> k_{ISC}$, k_T) as reported previously.[8] Thus, we demonstrated that since the addition of KI changed the triplet-state parameters, the triplet state kinetics were accurately investigated by the FCS measurements and analysis.

In PIT, it is suggested that the aggregation of the conjugates, which is involved in

physical damage to the cell membrane, may be induced via the triplet state of IR700. Here we showed that the calculated Φ_{ISC} of compound **1** was 0.019 ± 0.002. In comparison, the value is much lower than those of water-soluble silicon, aluminum, zinc, tin and germanium Pc derivatives (Φ_{ISC} = 0.44~0.68 in phosphate buffered saline (PBS)),[18] whereas the recently reported Φ_{ISC} of a silicon Pc derivative was very similar (Φ_{ISC} = 0.036 in PBS).[19] The former water-soluble Pc derivatives have a multivalent sulfonated Pc ring and the latter silicon Pc derivative is not substituted on the Pc ring. Since compound **1** is structurally similar with the latter silicon Pc derivative, the structural difference of the Pc ring may influence the Φ_{ISC}; however, further investigation is needed. The lower Φ_{ISC} of compound **1** suggests that the photocleavage reaction of the axial ligand on IR700 may be a very minor relaxation process. If so, it is possible that the cytotoxic effect of PIT in deep site of tumor can be improved by developing a light-sensitive PIT photosensitizer with a high Φ_{ISC}. One method to increase Φ_{ISC} is to introduce heavy atom, such as bromine and iodine, to phthalocyanine ring utilizing spin-orbit coupling by spin-orbit coupling.

4. Conclusion

In conclusion, we determined the Φ_{ISC} of an IR700 derivative using FCS. In the

FCS measurement with KI, triplet kinetic parameters were changed due to the heavy atom effect of iodine, demonstrating that the measurement was valid. The information on the Φ_{ISC} of the IR700 derivative should be useful for developing a novel photosensitizer for PIT.

CRediT authorship contribution statement

Hideo Takakura: Conceptualization, Methodology, Visualization, Writing - original draft, Funding acquisition. **Yuto Goto:** Investigation, Data curation, Visualization. **Akira Kitamura:** Conceptualization, Methodology, Formal analysis, Resources, Writing – review & editing, Funding acquisition. **Toshitada Yoshihara:** Investigation, Resources. **Seiji Tobita:** Resources, Writing - review & editing. **Masataka Kinjo:** Resources, Writing - review & editing. **Mikako Ogawa:** Conceptualization, Methodology, Writing - review & editing, Funding acquisition, Project administration.

Acknowledgments

We thank Tsumugi Kurosaki, Daisuke Yamashita, and Satoru Momosaki for supporting the FCS measurement. This work was supported by JST-PRESTO (Grant Number: JPMJPR15P5 to M.O.), JST-CREST (Grant Number: JPMJCR1902 to M.O.),

and by The Tokyo Biochemical Research Foundation (grant to H.T.). A.K. was supported by a Japan Society for Promotion of Science (JSPS) Grant-in-Aid for the Promotion of Joint International Research (Fostering Joint International Research) (16KK0156), by a JSPS Grant-in-Aid for Scientific Research (C) (18K06201); by a grant from Canon Foundation; by a Japan Science and Technology Agency (JST) Competitive Funding Program for Adaptable and Seamless Technology Transfer Program through Target-driven R&D (A-STEP) (VP30318089120).

References

1. M. Mitsunaga, M. Ogawa, N. Kosaka, L. T. Rosenblum, P. L. Choyke and H. Kobayashi, *Nat Med*, 2011, **17**, 1685-1691.
2. N. Shirasu, H. Yamada, H. Shibaguchi, M. Kuroki and M. Kuroki, *Int J Cancer*, 2014, **135**, 2697-2710.
3. H. Kobayashi and P. L. Choyke, *Acc Chem Res*, 2019, **52**, 2332-2339.
4. M. Ogawa, Y. Tomita, Y. Nakamura, M. J. Lee, S. Lee, S. Tomita, T. Nagaya, K. Sato, T. Yamauchi, H. Iwai, A. Kumar, T. Haystead, H. Shroff, P. L. Choyke, J. B. Trepel and H. Kobayashi, *Oncotarget*, 2017, **8**, 10425-10436.
5. K. Nakajima, H. Takakura, Y. Shimizu and M. Ogawa, *Cancer Sci*, 2018, **109**, 2889-2896.
6. K. Sato, K. Ando, S. Okuyama, S. Moriguchi, T. Ogura, S. Totoki, H. Hanaoka, T. Nagaya, R. Kokawa, H. Takakura, M. Nishimura, Y. Hasegawa, P. L. Choyke, M. Ogawa and H. Kobayashi, *ACS Cent Sci*, 2018, **4**, 1559-1569.
7. C. G. Hübner, A. Renn, I. Renge and U. P. Wild, *J Chem Phys*, 2001, **115**, 9619-9622.
8. J. Widengren, U. Mets and R. Rigler, *J Phys Chem*, 1995, **99**, 13368-13379.
9. H. Blom, A. Chmyrov, K. Hassler, L. M. Davis and J. Widengren, *J Phys Chem A*, 2009, **113**, 5554-5566.
10. J. Stromqvist, A. Chmyrov, S. Johansson, A. Andersson, L. Maler and J. Widengren, *Biophys J*, 2010, **99**, 3821-3830.
11. K. Suzuki, A. Kobayashi, S. Kaneko, K. Takehira, T. Yoshihara, H. Ishida, Y. Shiina, S. Oishi and S. Tobita, *Phys Chem Chem Phys*, 2009, **11**, 9850-9860.
12. R. Rigler, Ü. Mets, J. Widengren and P. Kask, *Euro Biophys J*, 1993, **22**.
13. J. R. Lakowicz, *Principles of fluorescence spectroscopy*, Springer, New York, N.Y., 3rd ed edn., 2006.
14. J. Widengren, R. Rigler and U. Mets, *J Fluoresc*, 1994, **4**, 255-258.
15. A. Chmyrov, T. Sanden and J. Widengren, *J Phys Chem B*, 2010, **114**, 11282-11291.
16. C. D. Geddes, *Measurement Science and Technology*, 2001, **12**, R53-R88.
17. M. Montalti and S. L. Murov, *Handbook of Photochemistry*, CRC Press, Boca Raton, Fl, 2006.
18. A. Ogunsipe and T. Nyokong, *Photochem Photobiol Sci*, 2005, **4**, 510-516.
19. E. D. Anderson, S. Sova, J. Ivanic, L. Kelly and M. J. Schnermann, *Phys Chem Chem Phys*, 2018, **20**, 19030-19036.

Figures

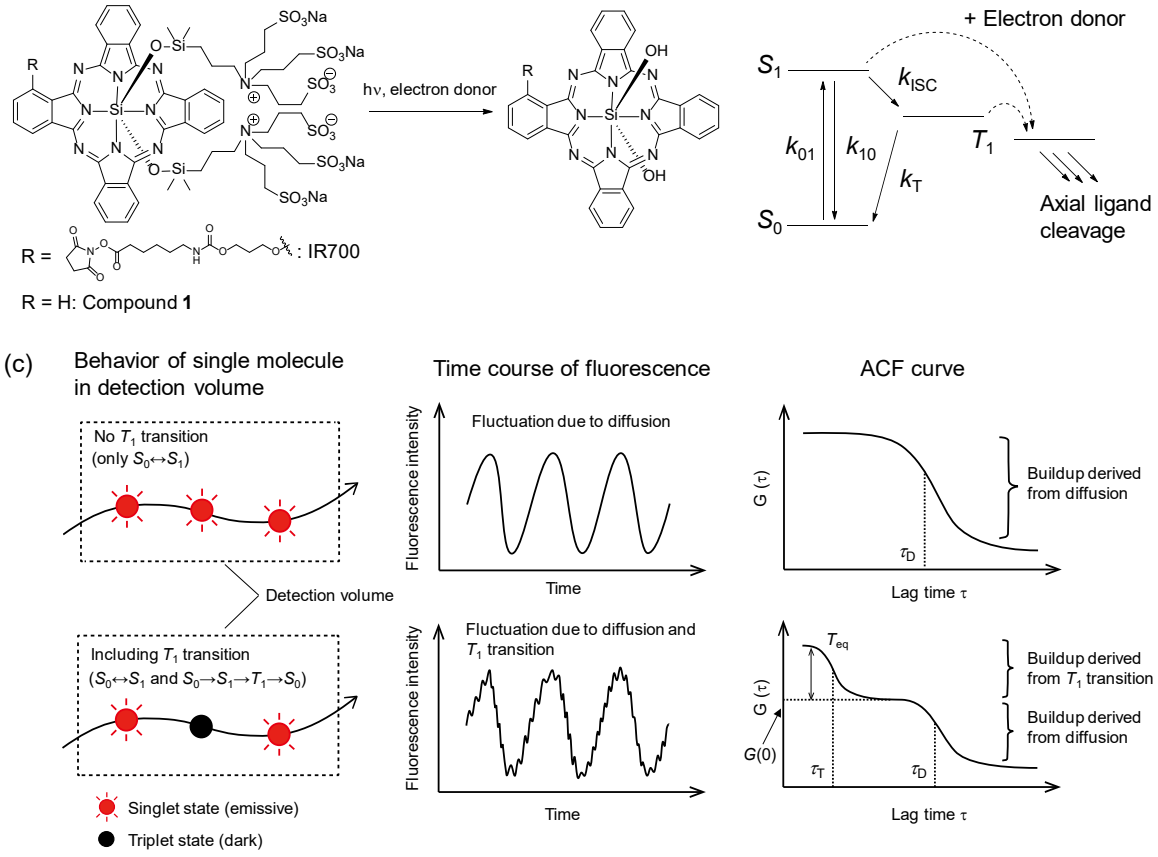

Fig. 1. (a) Photocleavage reaction of IR700 and compound **1**. The axial ligands of the compounds are cleaved by NIR light irradiation in the presence of an electron donor, yielding a hydrophobic product. (b) Photoexcited state model including the photocleavage reaction. k_{01} and k_{10} denote the rates of excitation from S_0 to S_1 and relaxation from S_1 to S_0, respectively. k_{ISC} and k_T denote the rates of intersystem crossing from S_1 to T_1 and triplet relaxation from T_1 to S_0, respectively. (c) Principle of FCS analysis. In FCS, excited molecules in the detection volume emit fluorescence. When the

excited molecule relaxes from S_1 to S_0, it emits photons at the nanosecond order, and the fluorescence intensity fluctuates with time due to in-and-out of the molecules in the detection volume through their diffusion. As a result, the buildup of the amplitude in ACF is observed (upper row). On the other hand, when a T_1 transition occurs during the passage through the volume, the fluorescence emission of the molecule is prohibited while staying in T_1; then, the fluorescence intensity fluctuates with the T_1 transition time, *i.e.* blinking time, in addition to the fluctuation derived from the diffusion. Usually, the time range of the T_1 transition is shorter than that of diffusion; therefore, the blinking and diffusion time constants can be distinguished as different decay times in the ACF (τ_T and τ_D, respectively). Moreover, in addition to the amplitude derived from diffusion ($G(0)$), one more amplitude corresponding to the blinking fraction can be observed in the ACF (blinking population at equilibrium: T_{eq}) (lower row).

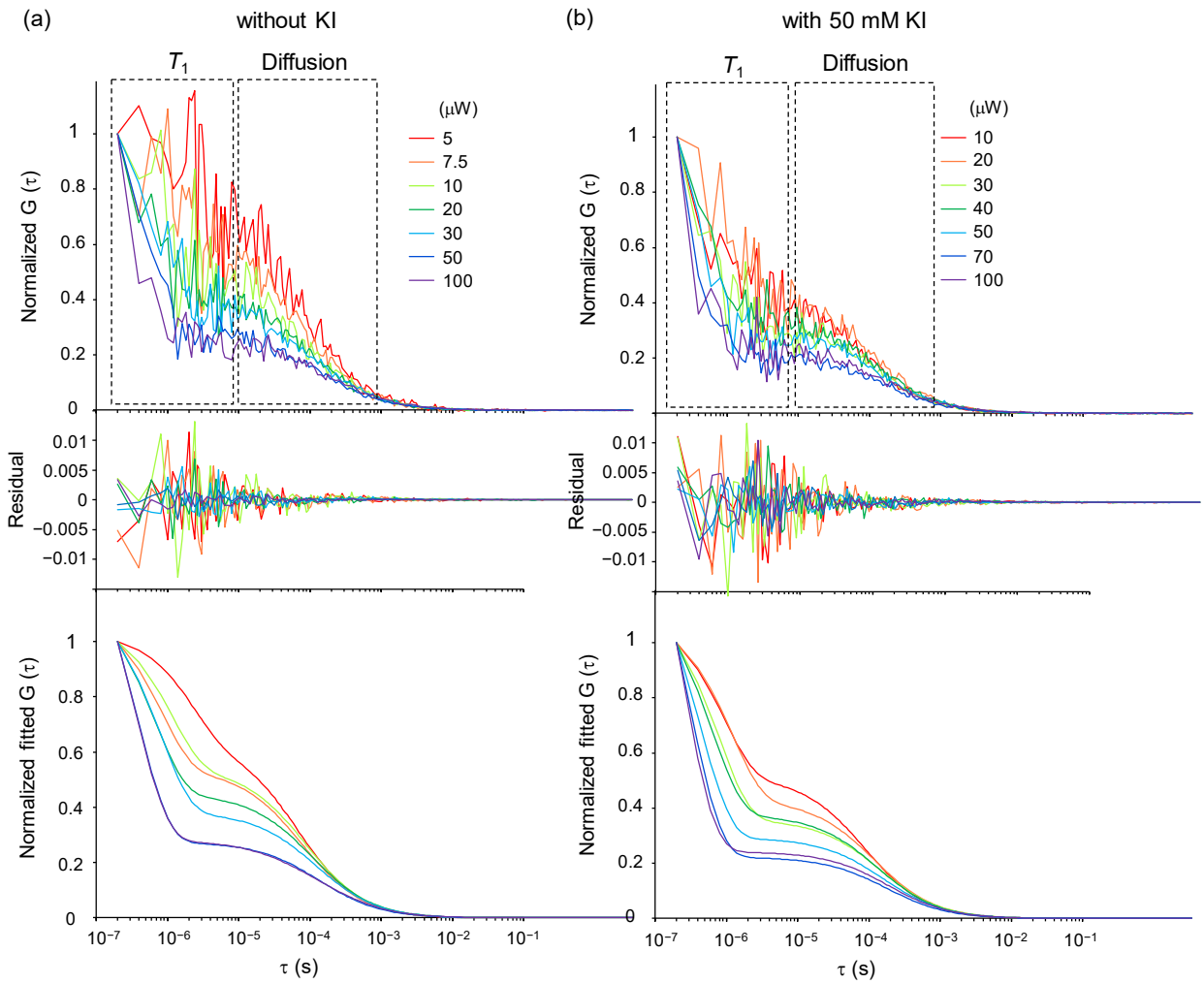

Fig. 2. (a, b) ACF curves of compound **1** at various excitation powers in the absence and presence of 50 mM KI. The ACFs were normalized at 0.2 μs. The amplitudes derived from T_1 and diffusion are indicated. The residuals and fitted ACF curves are also shown.

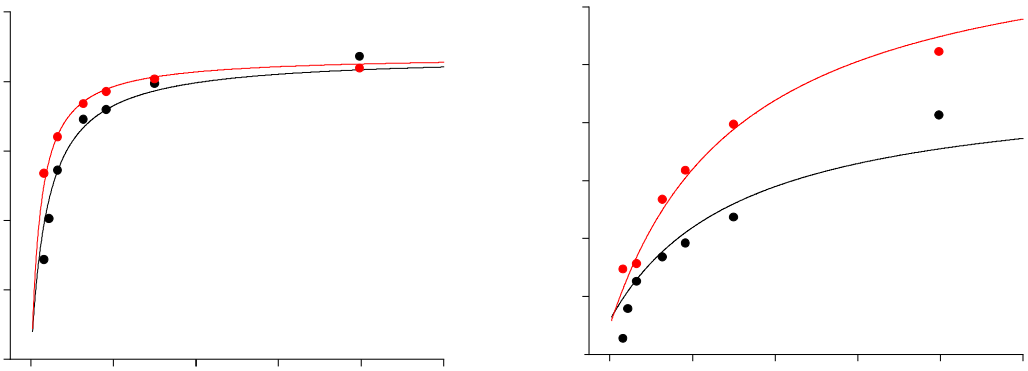

Fig. 3. Typical fitting plots of (a) a blinking population at equilibrium (T_{eq}) and (b) exponential relaxation rate obtained in Fig. 2 against the excitation powers.

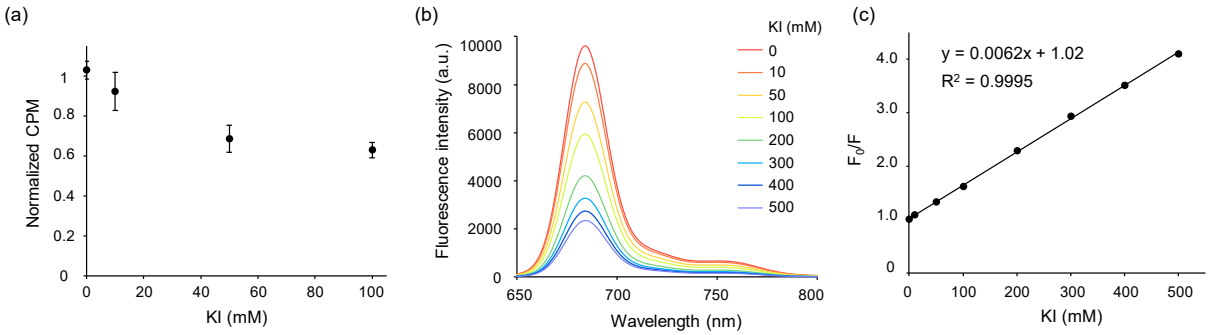

Fig. 4. (a) Decrease of brightness of compound **1** with various concentrations of KI using counts per molecule (CPM) obtained from FCS. The CPM values were normalized with that observed without KI addition. (b) Fluorescence spectra of compound **1** with various concentrations of KI. (c) Stern-Volmer plot of compound **1** against KI concentration. The fluorescence intensity of compound **1** at 684 nm in Fig. 4b was used for the plot.

Table 1. Triplet state-related kinetic parameters and photochemical properties of compound **1**.

	$k_{ISC}/\mu s^{-1}$	$k_T/\mu s^{-1}$	Φ_{FL}	Φ_{ISC}	τ_{FL}/ns
compound **1**	3.8 ± 0.3	0.56 ± 0.04	0.31	0.019 ± 0.002	4.9
+ 50 mM KI	5.9 ± 1.0*	0.54 ± 0.04			
+ 100 mM KI	6.3 ± 0.5*	0.51 ± 0.02			

Data represented as mean ± SD (n = 3–5). The statistical significance of the addition of KI compared to the absence of KI was assessed by a two-tailed student *t*-test assuming equal variances, $*p < 0.005$.

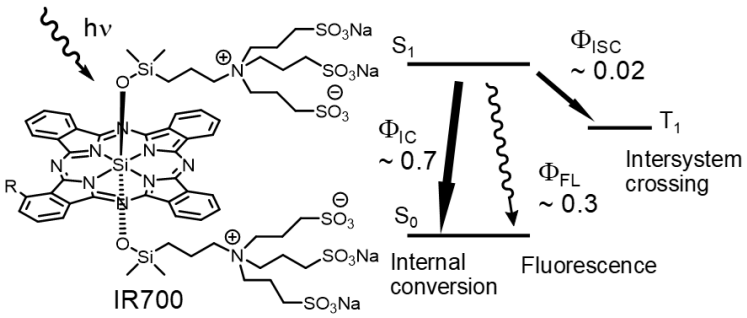

Graphical abstract